HHS Public Access

Author manuscript

Cell Rep. Author manuscript; available in PMC 2018 August 08.

Published in final edited form as:

Cell Rep. 2017 August 08; 20(6): 1287–1294. doi:10.1016/j.celrep.2017.07.034.

A Soluble Fluorescent Binding Assay Reveals PIP_2 Antagonism of TREK-1 Channels

Cerrone Cabanos[1], **Miao Wang**[2], **Xianlin Han**[2], and **Scott B. Hansen**[1,3,*]

[1]Departments of Molecular Medicine and Neuroscience, The Scripps Research Institute, Jupiter, FL 33458, USA

[2]Center for Metabolic Origins of Disease, Sanford Burnham Prebys Medical Discovery Institute, 6400 Sanger Road, Orlando, FL 32827, USA

SUMMARY

Lipid regulation of ion channels by low-abundance signaling lipids phosphatidylinositol 4,5-bisphosphate (PIP_2) and phosphatidic acid (PA) has emerged as a central cellular mechanism for controlling ion channels and the excitability of nerves. A lack of robust assays suitable for facile detection of a lipid bound to a channel has hampered the probing of the lipid binding sites and measuring the pharmacology of putative lipid agonists for ion channels. Here, we show a fluorescent PIP_2 competition assay for detergent-purified potassium channels, including TWIK-1-related K^+-channel (TREK-1). Anionic lipids PA and phosphatidylglycerol (PG) bind dose dependently (9.1 and 96 mM, respectively) and agonize the channel. Our assay shows PIP_2 binds with high affinity (0.87 mM) but surprisingly can directly antagonize TREK-1 in liposomes. We propose a model for TREK-1 lipid regulation where PIP_2 can compete with PA and PG agonism based on the affinity of the lipid for a site within the channel.

Graphical abstract

*Correspondence: shansen@scripps.edu.

[3]Lead Contact

SUPPLEMENTAL INFORMATION

Supplemental Information includes Supplemental Experimental Procedures, five figures, and one table and can be found with this article online at http://dx.doi.org/10.1016/j.celrep.2017.07.034.

AUTHOR CONTRIBUTIONS

S.B.H. and C.C. designed the experiments and wrote the manuscript. C.C. performed all the experiments except for the shotgun lipidomics, which was performed by M.W. and analyzed by X.H. and S.B.H.

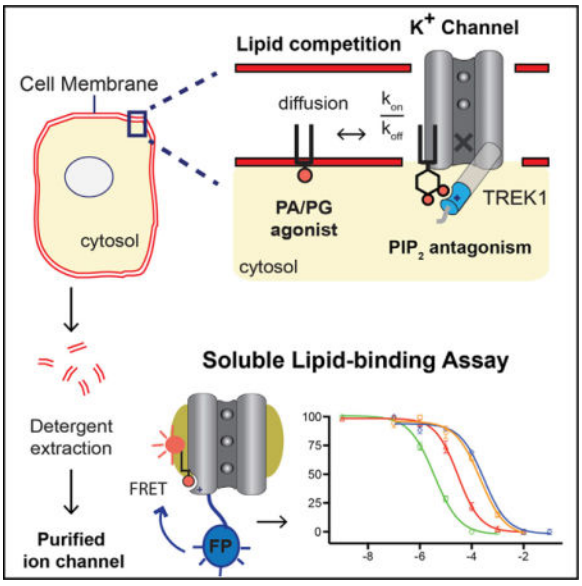

INTRODUCTION

Tandem of pore domains in a weak inward rectifying K^+ channel (TWIK)-1-related K^+-channel (TREK-1) is a two-pore domain potassium channel (K2P) expressed throughout the brain and peripheral nervous system (Fink et al., 1996). Small to medium sensory neurons in the dorsal root ganglion (DRG) express high levels of TREK-1, and this expression gives rise to a hyperpolarizing background current that works opposite nociceptive channels (e.g., transient receptor potential cation channel subfamily V member 1 [TRPV1] channels; Alloui et al., 2006) to suppress pain (Li and Toyoda, 2015). Stretch, swelling, poly-unsaturated fatty acids (PUFAs), volatile anesthetics (Enyedi and Czirják, 2010; Honoré et al., 2002; Maingret et al., 2000; Noël et al., 2009; Patel and Honoré, 2001), and the anionic signaling lipids phosphatidylinositol 4,5-bisphosphate (PIP_2) and phosphatidic acid (PA) are thought to regulate TREK-1 (Chemin et al., 2005; Comoglio et al., 2014; Lopes et al., 2005). In addition to TREK-1, anionic lipids regulate numerous ion channels that control cell membrane potential, permeability, and excitability (Hansen, 2015; Hille et al., 2015; Suh and Hille, 2008).

Recently, structural and biochemical studies have shown that anionic signaling lipids directly bind to and gate ion channels (Gamper and Shapiro, 2007; Hansen, 2015; Hansen et al., 2011; Svobodova and Groschner, 2016; Whorton and MacKinnon, 2011). For example, PIP_2 and PA bind tightly to a lipid binding site located within the transmembrane domain of the inward K^+ rectifier Kir2.2, gate the channel in a dose-dependent manner, and define the prototypical “lipid gating” of an ion channel (Hansen, 2015; Hansen et al., 2011). Also, PIP_2 inhibits TRPV1 by directly binding to a site in the transmembrane domain of the channel (Gao et al., 2016). Perturbations of anionic lipids in cell membranes regulate TREK-1 similar to Kir and TRPV1, suggesting lipids may bind directly to a site in TREK-1 (Chemin et al., 2005, 2007). Supporting this hypothesis, a recent crystal structure revealed the primary residues that conveyed PIP_2 sensitivity are in a structured α helix extending from

the fourth transmembrane domain (M4) helix (Dong et al., 2015) (PDB: 4XDK, D subunit) (see Figure S1).

However, which lipids bind and whether they agonize or antagonize the channel remains unclear. PA appears to activate TREK-1 as phospholipase D2 (PLD2) directly binds to TREK-1 and activates the channel through local production of lipid (Comoglio et al., 2014). PIP_2 regulation of TREK-1 is more complex; initially, PIP_2 was thought to activate the channel, and G_q depletion of PIP_2 inactivated the channel (Kang et al., 2006; Lopes et al., 2005). But later studies showed increasing PIP_2 after activation inhibits TREK-1 (Chemin et al., 2007). To identify lipid ligands and measure the affinities of lipids directly binding to potassium channels, we developed a simple mix-and-read fluorescent lipid binding assay amenable to TREK-1, TWIK-related arachidonic acid activated K^+ channel (TRAAK), Kir2.1, and Kir2.2 channels. We show that PIP_2 directly binds to TREK-1 and competes with lipid agonists PA and phosphatidylglycerol (PG) in purified liposomes. These data, combined with previous studies of PLD2 activation of TREK-1 (Comoglio et al., 2014), led us to propose a model where PIP_2 can directly antagonize TREK-1.

RESULTS

Development of a Lipid Binding Assay

To test PIP_2 binding to TREK-1, we fused a nanoluciferase (Nluc) to the C terminus of the channel and identified a soluble fluorescent PIP_2 (FL-PIP_2) analog suitable for binding to TREK-1. Figure 1A shows a cartoon of the assay design. Activation of Nluc produced an FL-PIP_2-dependent bioluminescence resonance energy transfer (BRET) signal specific to TREK-1 (Figure 1B). When directly titrated, the soluble FL-PIP_2 probe bound TREK-1 with a dissociation constant (K_d) of 1.6 μM and a Hill slope of 1.35 (Figure 1C).

In addition to TREK-1, FL-PIP_2 bound to purified Kir2.2, Kir2.1, and TRAAK channels (Figure 1B). As mentioned, Kir2.2 has known direct binding of PIP_2 to the transmembrane domain at the cytoplasmic interface (Hansen et al., 2011). TRAAK is also thought to bind PIP_2 (Enyedi and Czirják, 2010). Kir2.2 had the highest affinity for PIP_2 at 120 nM followed by Kir2.1, TREK-1, and TRAAK. As a negative control, we tested FL-PIP_2 binding to G protein inward-rectifying potassium channel (GIRK/Kir3.2). GIRK is a Kir2 homolog, but only weakly binds PIP_2 in the absence of G protein (>30 μM) (Whorton and MacKinnon, 2011). As expected, we saw no significant binding of FL-PIP_2 up to 10 μM (Figures 1B and 1C). The assay also worked using a FRET-based assay with GFP (Figure S2A), albeit it required 100 times the protein as the BRET assay (100 nM versus 1.0 nM).

To eliminate the potential artifacts from the luciferase enzyme or the fluorophore attached to the probe, we confirmed PIP_2 binding to TREK-1 in a radioactive version of the lipid binding assay using a tritiated (^3H) PIP_2 and a scintillation proximity assay (SPA). Figure 1D shows binding of ^3H-PIP_2 to detergent-purified TREK-1 channel; FL-PIP_2 dose-dependently competed with ^3H-PIP_2 (K_d, 0.80 μM; Hill slope, −0.85) (see also Figure S2C).

Pharmacology of Endogenous Membrane Lipids

We rapidly screened the binding of endogenous cellular lipids to four potassium channels and identified high-affinity lipid ligands. PA and PIP_2 bound with varying affinity to TREK-1, TRAAK, Kir2.2, and Kir2.1 (Figures 1E and 1F). We determined a K_d for each lipid by fitting the data to a sigmoidal dose-response curve with variable slope (GraphPad Prism). Head group composition drove TREK-1 lipid specificity for both soluble short chain (Figure S2D) and native membrane lipids (Figures 2A and 2B). PA and PIP_2 consistently bound the tightest (Table S1). The zwitterionic lipids 8:0 phosphatidylethanolamine (PE) and 8:0 phosphatidylcholine (PC) had no affinity for TREK-1 (Figure S2C).

Application of 10 μM arachidonic acid (AA) (free fatty acid) to cells expressing TREK-1 robustly activates TREK-1 (Patel et al., 1998). We tested for direct binding of AA to TREK-1 and found both ω-3 and ω-6 AA (free fatty acid) competed with FL-PIP_2 (Figure 2C). Fatty acid binding was highly specific because eicosapentaenoic acid (EPA, 20:5 ω-3) and saturated fatty acids failed to bind (Figure 3C). The K_ds for free ω-3 and ω-6 AAs were relatively weak, 67.1 ± 10.8 μM and 73.1 ± 12.1 μM, respectively (Figure 3D; Table S1), suggesting phospholipid incorporation into the membrane may also contribute to the activation of TREK-1.

Incorporation of AA into nociceptive membrane directly modulates touch through arachidonyl-containing membrane lipids (Vásquez et al., 2014). If the arachidonyl acyl chains of activating lipids bind directly to the channel, this could increase the affinity and further activate the channel. Using our BRET assay, we found arachidonic-acid-containing PA (AA-PA) (18:0–20:4) bound 2-fold tighter compared with 18:1 PA (9.1 μM versus 15.8 μM; $p = 0.0423$). AA-PA was also statistically a higher affinity than 16:0–18:1 PA ($p = 0.0356$). This was not true of arachidonyl PIP_2 (18:0–20:4) (Figures S3A and S3B; Table S1). Complete removal of an acyl chain had the greater affect. TREK-1 affinity for lyso-PA decreased 3.5-fold compared with diacyl (18:1) PA (56.0 μM versus 15.8 μM) (see also Table S1). Shotgun lipidomics of HEK cells treated with 50 μM AA showed an ~10- and 3-fold increase in arachidonyl PG and PA, respectively, further supporting a role for arachidonyl-containing phospholipid in TREK-1 activation (Figure S4A).

Lastly, we tested the contribution of the glycerol backbone to TREK-1 affinity. Ceramide-1-phophate (C1P) is often a saturated lipid with an identical head group as PA and differs only in the acyl chain linkage (Figures S3E–S3G). We found C1P binding to TREK-1 was 4-fold weaker than PA (79.4 μM versus 19.6 μM; 8:0 and 16:0 lipids were similar). The Hill coefficients were near 1.0 for each lipid. Furthermore, lyso-C1P, i.e., sphingosine-1-phosphate (S1P), had no affinity at 100 μM (Table S1). These results suggest the acyl chain and backbone combine to give high-affinity lipid binding in TREK-1. Also, the chemical specificity suggests a structurally well-defined lipid binding site.

Lipid Gating of TREK-1

To determine whether PG, PA, and PIP_2 are TREK-1 agonists or antagonists, we tested ion conductance in a flux assay (Brohawn et al., 2012). PA and PG are both products of the enzyme PLD2 (Yang et al., 1967), and we expect these lipids to agonize the channel as

PLD2 binds directly to the C terminus of TREK-1 and activates the channel (Comoglio et al., 2014) (see also Figure S5). 5–15 mol% PG dose-dependently activated TREK-1 in 1,2-dioleoyl-sn-glycero-3-phosphocholine (DOPC) liposomes, as determined by potassium ion flux (Figures 3A and 3B). PG is relatively abundant in the plasma membrane, and the low affinity is appropriate for agonizing the channel. The flux assay assumes equal incorporation of the channel between lipid types. We confirmed TREK-1 incorporation into the liposome using fluorescence from a GFP tag on TREK-1 (Figure 3I). In PG liposomes, the fluorescence was similar, suggesting the effect of PG on TREK-1 is a lipid-specific interaction. PA likewise activated the channel, albeit with less flux (Figure 3C). Incorporation of TREK-1 appeared to increase with 15 mol% PA compared with 10 mol% (the GFP fluorescence increased to 17,800 RU; $p = 0.02$, unpaired Student's t test). Hence, some of the increased PA activation may be an artifact of increased TREK-1 incorporation. In contrast with PG and PA, increasing concentrations of PIP_2 (0.5, 1, and 2 mol%) failed to activate TREK-1: the highest concentration of PIP_2, 2 mol%, induced the least flux (Figures 3E and 3F). Given that our soluble binding assay shows that PIP_2 binds the channel, we reasoned PIP_2 could bind and antagonize TREK-1.

To determine antagonistic properties of PIP_2 on TREK-1, we combined increasing concentration of PIP_2 with 10% PG, a concentration of PG that opens the channel (Figure 3A, blue trace). Consistent with antagonism, TREK-1 currents were completely inhibited in 5 mol% PIP_2 (Figure 3C), as were channels in 2 mol%. Unexpectedly, sub-saturating PIP_2 (0.5 mol%) in the presence of 10 mol% PG enhanced TREK-1 activity (Figures 3G and 3H). Reconstitution efficiency of TREK-1 into the liposomes does not account for the increased flux because the incorporation in 0.5 mol% differed from 5 mol% by less than 20% (Figure 3I), but flux increased 7-fold.

To further confirm that the lipid K_d arises from the signaling lipid directly binding to structured protein, we mutated residues in the distal end of the M4 helix, a site previously implicated in lipid binding based on electrophysiology experiments (Chemin et al., 2005). Consistent with direct lipid binding, we found mutating R297 to cysteine completely blocked 500 nM ^{3}H-PIP_2 binding to TREK-1 (Figure 4A). To confirm the functionality of this cysteine mutant, we tested channel conductance in our ion flux assay. To do this, we made a partner double-cysteine mutation, F171C + R297C (cysTREK), to trap the channel in a disulfide bonded or "lipid-bound" (active) conformation when oxidized, analogous to a pair of cys mutants previously characterized in TRAAK channels using whole-cell patch clamp (Brohawn et al., 2014a) (see Figure S1). Like patch clamp, cysTREK in liposomes rescued flux activity when oxidized; but when the disulfides were reduced, the channel's flux significantly decreased, consistent with low-affinity agonist binding (Figure 4C). We confirmed a 10-fold loss in lipid binding affinity using our BRET assay (Figure 4B).

Lastly, we investigated the ability of TREK-1 small-molecule antagonists norfluoxetine (Dong et al., 2015) (NFX), fluphenazine (Thümmler et al., 2007) (FLZ), and thioridazine (Thümmler et al., 2007) (TRZ) to compete with FL-PIP_2 binding. FLZ bound tightly to TREK-1 with a K_d of 6.5 ± 2.0 μM, followed by TRZ of 52.7 ± 5.5 μM, and NFX of 68.2 ± 14.0 μM (Figure 4D). Also, binding was channel specific because PIP_2 binding to TRAAK was unaffected by TRZ (Figure S4B), in agreement with previous studies (Thümmler et al.,

2007). Because PIP_2 appears to antagonize TREK-1, it is unclear whether binding of small molecules is directly competing or if there are multiple conformations that lead to antagonism. Interestingly, FLZ appeared to bind non-competitively because 40% of FL-PIP_2 remained bound at what appeared to be near-saturating concentrations (Figure 4D).

DISCUSSION

Taken together, the nanomolar affinity for PIP_2, the specificity for the glycerol backbone and acyl chains, and the agonism by anionic lipids (PA or PG) solidify a high-affinity lipid binding site within TREK-1. Figure 4E shows a proposed model for lipid gating in TREK-1. The PIP_2 affinity for TREK-1 (860 nM) is only slightly weaker than Kir2.1 (450 nM) and suggests that structural determinants like Kir2.2 exist (Hansen, 2015; Hansen et al., 2011).

We directly measured the functional effect of PIP_2 on TREK-1 channels in a purified reconstituted system (Figure 3A). The purified system is critical to determining the direct effect of a lipid, because whole cells are confounded by indirect effects of PIP_2. For example, PIP_2 can activate PLD2 (Lopez et al., 1998), which would indirectly agonize TREK-1 through the generation of PA (see Figure S5A), yet appear as activation by PIP_2. The lateral distribution of lipids varies dramatically (Simons and Sampaio, 2011) in a membrane, and measuring the precise concentration of lipids near a channel is difficult (Hansen, 2015). This limits our ability to correlate the antagonism in our purified system with exact relevant lipid concentrations in a biological membrane. However, crude increases in PIP_2 concentration after initial activation have been shown to inactivate TREK-1 in cell culture (Chemin et al., 2007), consistent with our direct PIP_2 antagonism playing a role in vivo.

The opposite effect of low and high levels of PIP_2 in the presence of PG (Figures 3G and 3H) may suggest multiple sites for PIP_2 binding to TREK-1. TREK-1 is a pseudotetramer (dimer of dimer) and could have two distinct lipid binding sites (one agonizing and one antagonizing). If so, agonizing lipids PA and PG could compete with PIP_2 through an allosteric mechanism at distinct sites. Alternatively, the dimer could have only one PIP_2 site (two per dimer) and only antagonize when both sites of the dimer are bound. At sub-saturating concentrations, the presence of PIP_2 would give the appearance of higher anionic lipid concentration but lack a sufficient concentration to occupy both PIP_2 sites, thus failing to antagonize the channel. This effect resembles Kir, a homotetramer, which is activated when sub-saturating PA is added to agonizing PIP_2 (Cheng et al., 2011; Hansen, 2015). At high concentrations, PA competes off PIP_2 and antagonizes Kir (Hansen et al., 2011; Lee et al., 2013). As mentioned, PIP_2 could also indirectly activate TREK-1 through the enzyme PLD2. We recently showed PLD2 necessarily translocates to PIP_2 during activation (Petersen et al., 2016). These findings combined with Comoglio's model of localization of PLD2 in the activation of TREK-1 (Comoglio et al., 2014) suggest PIP_2 could indirectly activate TREK-1 through increasing PLD2 activation and production of PA and PG agonists (see Figure S5A). This later mode of action assumes PIP_2 must bind PLD2 with higher affinity than TREK-1, which is not known. A comparison of these two modes of activation is shown in Figure S5A, (i) and (ii). Distinguishing their relative contributions will require

further investigation. The expected changes in cellular lipid concentration relative to TREK-1 activity are modeled in Figure S5B.

The large selective increase of arachidonyl-PG (Figure S4A) with AA treatment may indicate PG-specific regulation of TREK-1. However, the addition of AA to cells can activate TREK-1 in seconds (Patel et al., 1998), and our lipidomics study incorporated AA over 15 min. Furthermore, free AA increases TRAAK currents in liposomes (Brohawn et al., 2014b). Additional experiments with sufficient temporal resolution are needed to better define the role of free AA in TREK-1 activation.

So why does PIP_2 antagonize TREK-1 in liposomes when PA and PG are activating? All three lipids are anionic. Inhibition by a cellular feedback mechanism is impossible in our purified (cell-free) liposomes. Rather, a structural or biophysical feature must explain the functional selectivity. Recent crystal structures of TREK-1 and TRAAK suggested that the lipid binding site, i.e., the distal end of the M4 helix[21], can move toward the membrane in the active conformation (Brohawn et al., 2014a; Dong et al., 2015; Lolicato et al., 2014) (Figure S1). The span of the inositol head group is substantial, 8.1 Å (see PIP_2 in Figure S2B), and could displace the most distal charges by positioning the anionic phosphate ~8 Å away from the membrane (Figure 4E; Figure S2B, PIP_2 chemical structure). This model is consistent with the previous up/down activating models established through double-cysteine mutants of TRAAK (Brohawn et al., 2014a). Conceivably, a thinner membrane could allow PIP_2 to shift up relative to the TREK-1 and allow the lipid binding site to sit closer to the active conformation. Gain-of-function mutations in TRAAK appeared to destabilize the TM4 helix prior to the lipid binding motif (Lolicato et al., 2014), which could also allow the lipid binding motif to associate with the membrane (move up), although the key residues were not visible in the pertinent structures (Lolicato et al., 2014; Miller and Long, 2012).

We conclude that lipid agonists and antagonists dually and directly contribute to gating of TREK-1 by binding with high affinity to the channel. We also demonstrate a simple mix-and-read fluorescent assay that accurately characterizes lipid specificity and affinities of a lipid bound to an ion channel. The state-dependent selectivity combined with the small requirement for protein make our soluble assay amenable to ultrahigh-throughput drug screening (2–3 million compounds). Our assay could be combined with high-throughput functional screens (200,000–300,000 compounds) (Su et al., 2016), which would allow a complete strategy for screening of ion channel in a purified system using techniques analogous to soluble proteins.

EXPERIMENTAL PROCEDURES

Protein Expression and Purification

TREK-1, TRAAK, Kir2.1, Kir2.2, or Kir3.2 (GIRK) containing a C-terminal fluorescent protein (either GFP or Nluc) with 103-His tag was expressed in *Pichia* yeast. After cryo-milling, the proteins were extracted in dodecyl-β-D-maltoside (DDM) with protease inhibitors and purified to homogeneity on a cobalt affinity column followed by size exclusion chromatography (SEC). The final SEC buffer contained 20 mM Tris (pH 8.0), 150 mM KCl, 1 mM EDTA, and 2 mM DDM. All proteins were expressed in milligram

quantities with a predominant monodispersed peak (Figure S4C) corresponding to the expected molecular weight (MW) of an assembled channel with a fluorescent tag in detergent.

BRET Lipid Binding Assay

The BRET was done in a 384-well plate, with each well having a total of 50 μL of total reaction volume consisting of 1 nM (binding sites) purified ion channel tagged with Nluc, 500 nM BODIPY-TMR phosphatidylinositol 4,5-bisphosphate (FL-PIP_2) (Echelon Biosciences), various concentrations of competing ligand, and 1:2,000 furimazine (NanoGlo; Promega), the substrate for Nluc, in the SEC buffer with 7 mM DDM final concentration. BRET signal brought about by the binding of FL-PIP_2 to TREK-1-Nluc and competition with a ligand was calculated by subtracting signal from Nluc-only control enzyme (purified from bacteria) and measured using Envision Multilabel 2104 plate reader (PerkinElmer) set for dual-emission detection (540 nm for Nluc and 574 nm for FL-PIP_2) and automatic BRET ratio calculation. Nluc control enzyme was purified from BL1 bacteria cells. Although not used here, background fluorescence can be determined using excess non-FL-PIP_2 (e.g., C8-PIP_2) rather than the Nluc control enzyme. Data points were fit to a sigmoidal dose-response curve with variable slope using GraphPad Prism. A FRET version of the assay employed a GFP tag rather than an Nluc tag. See also Figure S2A and Supplemental Experimental Procedures.

Radioactive Lipid Binding Assay

Binding of ^{3}H-PIP_2 to TREK-1 was detected in a SPA (Perkin Elmer). 100 nM TREK-1 binding sites was mixed in 0.6 mg/mL polyvinyltoluene (PVT) anti-mouse SPA beads, 0.8 μg/ml anti-His antibody, SEC buffer with 7 mM DDM, and a signal measured in a scintillation counter.

Potassium Flux Assay

Lipids of a desired ratio were mixed, dried, rehydrated, sonicated, and solubilized with 3 mM DDM. Proteoliposomes were formed by mixing 1:100 TREK-1/lipids and removal of detergent with BioBeads (150 mM KCl, 20 mM HEPES [pH 7.4]). Sonicated proteoliposomes (5 μL) were added to 195 μL of flux assay buffer (150 mM NaCl, 20 mM HEPES [pH 7.4], 2 μM 9-amino-6-chloro-2-methoxyacridine [ACMA]) in a 96-well plate at 25°C. Flux was initiated by the addition of the protonophore carbonyl cyanide *m*-chlorophenyl hydrazone (CCCP) (1 μM final concentration).

Shotgun Lipidomics

HEK293 cells were treated in 10 cm plates with 50 μM AA for 15 min. The cells were scraped and frozen for lipid extraction. The lipids were extracted using a modified Bligh and Dyer procedure (Han et al., 2012) and analyzed by electrospray ionization (ESI) direct infusion analysis (Yang et al., 2009).

Statistical Methods

All statistical calculations were performed in GraphPad Prism v6.0. For the Student's t test, significance was calculated using a two-tailed unpaired parametric test with significance defined as $p < 0.05$. For the multiple comparison test, significance was calculated using an ordinary one-way ANOVA and Tukey's multiple comparison test with a single pooled variance.

Supplementary Material

Refer to Web version on PubMed Central for supplementary material.

Acknowledgments

We thank Arman Nayebosadri for help with flux assays and Andrew Hansen for discussion and comments on the manuscript. This work was supported by a Director's New Innovator Award (1DP2NS087943-01 to S.B.H.) from the NIH.

References

Alloui A, Zimmermann K, Mamet J, Duprat F, Noël J, Chemin J, Guy N, Blondeau N, Voilley N, Rubat-Coudert C, et al. TREK-1, a K+ channel involved in polymodal pain perception. EMBO J. 2006; 25:2368–2376. [PubMed: 16675954]

Brohawn SG, del Mármol J, MacKinnon R. Crystal structure of the human K2P TRAAK, a lipid- and mechano-sensitive K+ ion channel. Science. 2012; 335:436–441. [PubMed: 22282805]

Brohawn SG, Campbell EB, MacKinnon R. Physical mechanism for gating and mechanosensitivity of the human TRAAK K+ channel. Nature. 2014a; 516:126–130. [PubMed: 25471887]

Brohawn SG, Su Z, MacKinnon R. Mechanosensitivity is mediated directly by the lipid membrane in TRAAK and TREK1 K+ channels. Proc Natl Acad Sci USA. 2014b; 111:3614–3619. [PubMed: 24550493]

Chemin J, Patel AJ, Duprat F, Lauritzen I, Lazdunski M, Honoré E. A phospholipid sensor controls mechanogating of the K+ channel TREK-1. EMBO J. 2005; 24:44–53. [PubMed: 15577940]

Chemin J, Patel AJ, Duprat F, Sachs F, Lazdunski M, Honore E. Up- and down-regulation of the mechano-gated K(2P) channel TREK-1 by PIP (2) and other membrane phospholipids. Pflugers Arch. 2007; 455:97–103. [PubMed: 17384962]

Cheng WWL, D'Avanzo N, Doyle DA, Nichols CG. Dual-mode phospholipid regulation of human inward rectifying potassium channels. Biophys J. 2011; 100:620–628. [PubMed: 21281576]

Comoglio Y, Levitz J, Kienzler MA, Lesage F, Isacoff EY, Sandoz G. Phospholipase D2 specifically regulates TREK potassium channels via direct interaction and local production of phosphatidic acid. Proc Natl Acad Sci USA. 2014; 111:13547–13552. [PubMed: 25197053]

Dong YY, Pike ACW, Mackenzie A, McClenaghan C, Aryal P, Dong L, Quigley A, Grieben M, Goubin S, Mukhopadhyay S, et al. K2P channel gating mechanisms revealed by structures of TREK-2 and a complex with Prozac. Science. 2015; 347:1256–1259. [PubMed: 25766236]

Enyedi P, Czirják G. Molecular background of leak K+ currents: two-pore domain potassium channels. Physiol Rev. 2010; 90:559–605. [PubMed: 20393194]

Fink M, Duprat F, Lesage F, Reyes R, Romey G, Heurteaux C, Lazdunski M. Cloning, functional expression and brain localization of a novel unconventional outward rectifier K+ channel. EMBO J. 1996; 15:6854–6862. [PubMed: 9003761]

Gamper N, Shapiro MS. Regulation of ion transport proteins by membrane phosphoinositides. Nat Rev Neurosci. 2007; 8:921–934. [PubMed: 17971783]

Gao Y, Cao E, Julius D, Cheng Y. TRPV1 structures in nanodiscs reveal mechanisms of ligand and lipid action. Nature. 2016; 534:347–351. [PubMed: 27281200]

Han X, Yang K, Gross RW. Multi-dimensional mass spectrometry-based shotgun lipidomics and novel strategies for lipidomic analyses. Mass Spectrom Rev. 2012; 31:134–178. [PubMed: 21755525]

Hansen SB. Lipid agonism: the PIP2 paradigm of ligand-gated ion channels. Biochim Biophys Acta. 2015; 1851:620–628. [PubMed: 25633344]

Hansen SB, Tao X, MacKinnon R. Structural basis of PIP2 activation of the classical inward rectifier K + channel Kir2.2. Nature. 2011; 477:495–498. [PubMed: 21874019]

Hille B, Dickson EJ, Kruse M, Vivas O, Suh BC. Phosphoinositides regulate ion channels. Biochim Biophys Acta. 2015; 1851:844–856. [PubMed: 25241941]

Honoré E, Maingret F, Lazdunski M, Patel AJ. An intracellular proton sensor commands lipid- and mechano-gating of the K(+) channel TREK-1. EMBO J. 2002; 21:2968–2976. [PubMed: 12065410]

Kang D, Han J, Kim D. Mechanism of inhibition of TREK-2 (K2P10.1) by the Gq-coupled M3 muscarinic receptor. Am J Physiol Cell Physiol. 2006; 291:C649–C656. [PubMed: 16672694]

Lee SJ, Wang S, Borschel W, Heyman S, Gyore J, Nichols CG. Secondary anionic phospholipid binding site and gating mechanism in Kir2.1 inward rectifier channels. Nat Commun. 2013; 4:2786. [PubMed: 24270915]

Li XY, Toyoda H. Role of leak potassium channels in pain signaling. Brain Res Bull. 2015; 119(Pt A): 73–79. [PubMed: 26321392]

Lolicato M, Riegelhaupt PM, Arrigoni C, Clark KA, Minor DL Jr. Transmembrane helix straightening and buckling underlies activation of mechanosensitive and thermosensitive K(2P) channels. Neuron. 2014; 84:1198–1212. [PubMed: 25500157]

Lopes CMB, Rohács T, Czirják G, Balla T, Enyedi P, Logothetis DE. PIP2 hydrolysis underlies agonist-induced inhibition and regulates voltage gating of two-pore domain K+ channels. J Physiol. 2005; 564:117–129. [PubMed: 15677683]

Lopez I, Arnold RS, Lambeth JD. Cloning and initial characterization of a human phospholipase D2 (hPLD2). ADP-ribosylation factor regulates hPLD2. J Biol Chem. 1998; 273:12846–12852. [PubMed: 9582313]

Maingret F, Patel AJ, Lesage F, Lazdunski M, Honore E. Lysophospholipids open the two-pore domain mechano-gated K(+) channels TREK-1 and TRAAK. J Biol Chem. 2000; 275:10128–10133. [PubMed: 10744694]

Miller AN, Long SB. Crystal structure of the human two-pore domain potassium channel K2P1. Science. 2012; 335:432–436. [PubMed: 22282804]

Noël J, Zimmermann K, Busserolles J, Deval E, Alloui A, Diochot S, Guy N, Borsotto M, Reeh P, Eschalier A, Lazdunski M. The mechano-activated K+ channels TRAAK and TREK-1 control both warm and cold perception. EMBO J. 2009; 28:1308–1318. [PubMed: 19279663]

Patel AJ, Honoré E. Properties and modulation of mammalian 2P domain K+ channels. Trends Neurosci. 2001; 24:339–346. [PubMed: 11356506]

Patel AJ, Honoré E, Maingret F, Lesage F, Fink M, Duprat F, Lazdunski M. A mammalian two pore domain mechano-gated S-like K+ channel. EMBO J. 1998; 17:4283–4290. [PubMed: 9687497]

Petersen EN, Chung HW, Nayebosadri A, Hansen SB. Kinetic disruption of lipid rafts is a mechanosensor for phospholipase D. Nat Commun. 2016; 7:13873. [PubMed: 27976674]

Simons K, Sampaio JL. Membrane organization and lipid rafts. Cold Spring Harb Perspect Biol. 2011; 3:a004697. [PubMed: 21628426]

Su Z, Brown EC, Wang W, MacKinnon R. Novel cell-free high-throughput screening method for pharmacological tools targeting K+ channels. Proc Natl Acad Sci USA. 2016; 113:5748–5753. [PubMed: 27091997]

Suh BC, Hille B. PIP2 is a necessary cofactor for ion channel function: how and why? Annu Rev Biophys. 2008; 37:175–195. [PubMed: 18573078]

Svobodova B, Groschner K. Mechanisms of lipid regulation and lipid gating in TRPC channels. Cell Calcium. 2016; 59:271–279. [PubMed: 27125985]

Thümmler S, Duprat F, Lazdunski M. Antipsychotics inhibit TREK but not TRAAK channels. Biochem Biophys Res Commun. 2007; 354:284–289. [PubMed: 17222806]

Vásquez V, Krieg M, Lockhead D, Goodman MB. Phospholipids that contain polyunsaturated fatty acids enhance neuronal cell mechanics and touch sensation. Cell Rep. 2014; 6:70–80. [PubMed: 24388754]

Whorton MR, MacKinnon R. Crystal structure of the mammalian GIRK2 K+ channel and gating regulation by G proteins, PIP2, and sodium. Cell. 2011; 147:199–208. [PubMed: 21962516]

Yang SF, Freer S, Benson AA. Transphosphatidylation by phospholipase D. J Biol Chem. 1967; 242:477–484. [PubMed: 6022844]

Yang K, Cheng H, Gross RW, Han X. Automated lipid identification and quantification by multidimensional mass spectrometry-based shotgun lipidomics. Anal Chem. 2009; 81:4356–4368. [PubMed: 19408941]

Highlights

- A soluble fluorescent assay directly measures lipid binding to potassium channels
- Lipids are direct ligands for two-pore domain potassium channels TREK and TRAAK
- Phosphatidic acid (PA) and phosphatidylglycerol (PG) agonize TREK-1
- Phosphatidylinositol 4,5 bisphosphate (PIP_2) can directly antagonize TREK-1

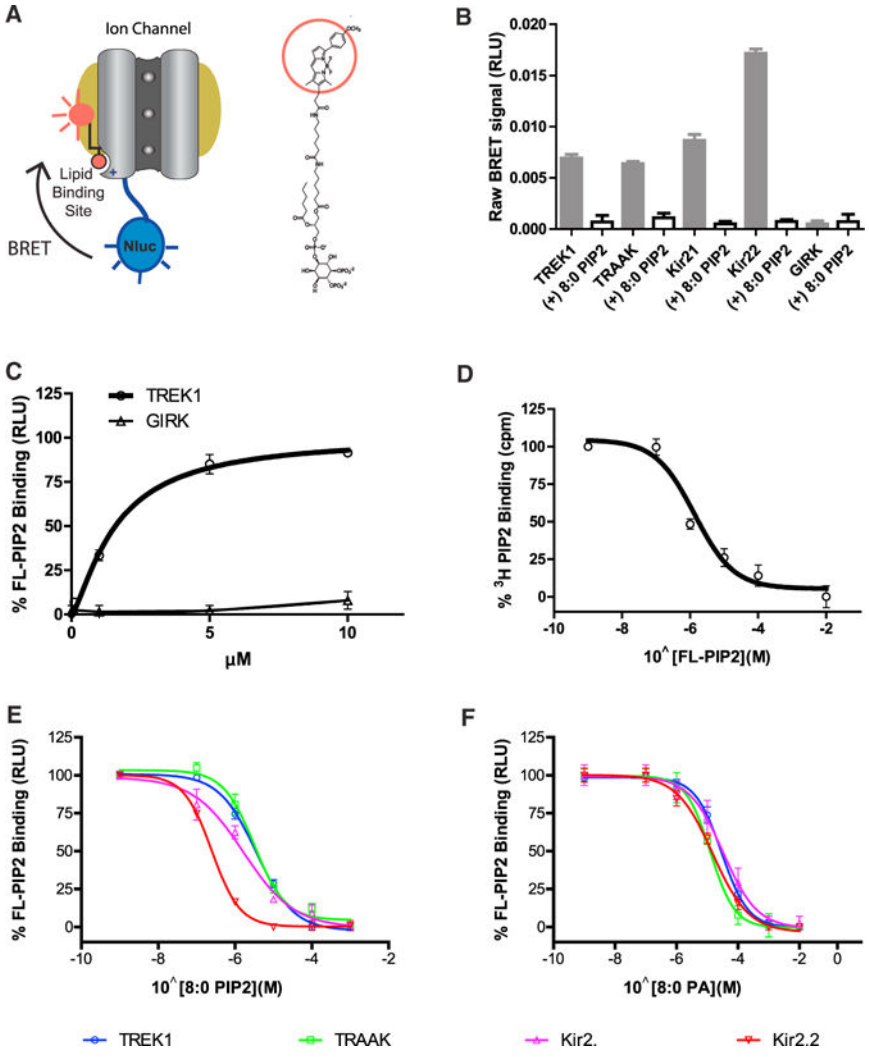

Figure 1. Soluble FL-PIP$_2$ Binding Assay to PIP$_2$ Channels

(A) Cartoon representation showing a single subunit of detergent-purified TREK-1 fused to the bioluminescent protein, Nluc. Excitation of bound FL-PIP$_2$ by Nluc produces a BRET-specific signal. A structure of FL-PIP$_2$ (right) labeled with BODIPY-TMR (red circle) (542/574 nm).

(B) Specific binding of FL-PIP$_2$ to TREK-1, TRAAK, Kir2.1, and Kir2.2 and competition with 100 μM non-fluorescent 8:0 PIP$_2$. No binding was observed for GIRK.

(C) Binding saturation curve of FL-PIP$_2$ to TREK-1 (K_d, 1.6 μM; Hill slope, 1.4).

(D) Dose-dependent competition of bound ^{3}H-PIP$_2$ (200 nM) with FL-PIP$_2$ (K_d, 0.8 μM; Hill slope, −0.9).

(E) 8:0 PIP$_2$ competition FL-PIP$_2$ for TREK-1 (K_d of 0.9 ± 0.1 μM), TRAAK (1.4 ± 0.3 μM), Kir2.1 (0.8 ± 0.2 μM), and Kir2.2 (0.1 ± 0.1 μM).

(F) 8:0 PA competes with K_d of 19.6 ± 2.9 μM for TREK-1, 8.5 ± 0.6 μM for TRAAK, 20.1 ± 5.6 μM for Kir2.1, and 29.1 ± 5.3 μM for Kir2.2.

Error bars represent SEM (n = 3–6). See also Figures S1 and S2 and Table S1.

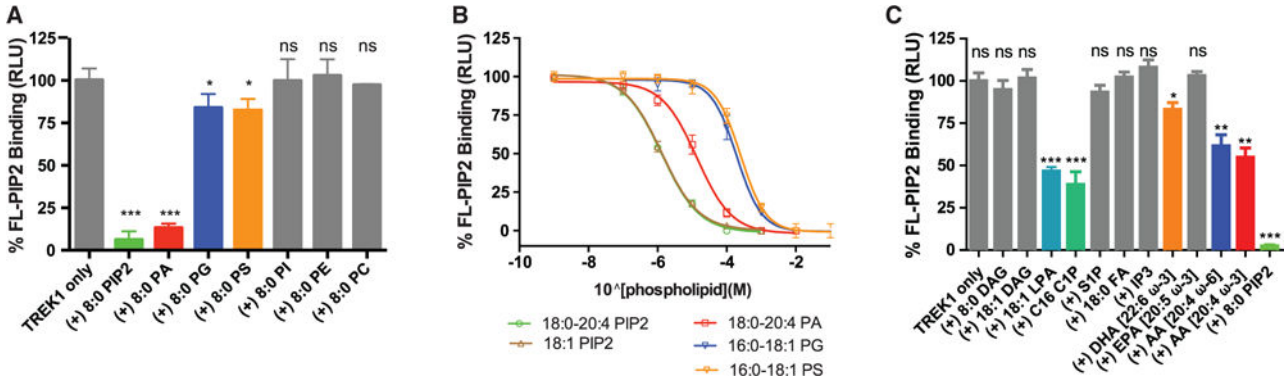

Figure 2. TREK-1 Pharmacology of Membrane Lipids

(A) Single-point competition of soluble lipids (100 μM) with FL-PIP_2 (500 nM) shows specificity for anionic lipids. Phosphatidylinositol (PI), PE, and PC do not compete for FL-PIP_2 binding.

(B) TREK-1 competition curves comparing head group specificity of full-length anionic lipids. PIP_2 binds with the highest affinity (K_d, 0.87 ± 0.11 μM). K_ds for 18:0–20:4 PIP_2 and 18:1–18:1 PIP_2 are indistinguishable.

(C) Single-point competition (100 μM) of FL-PIP_2 comparing cellular lipids with free fatty acids. The diacylglycerols (DAGs), 8:0 and 18:1 DAG, sphingosine-1-phosphate, stearic acid (18:0), inositol triphosphate (IP_3), and EPA (20:5) fail to compete off FL-PIP_2. ***$p < 0.0001$; **$p < 0.001$; *$p < 0.05$, Student's t test. Error bars represent SEM (n = 3–10). See also Figures S3–S5 and Table S1.

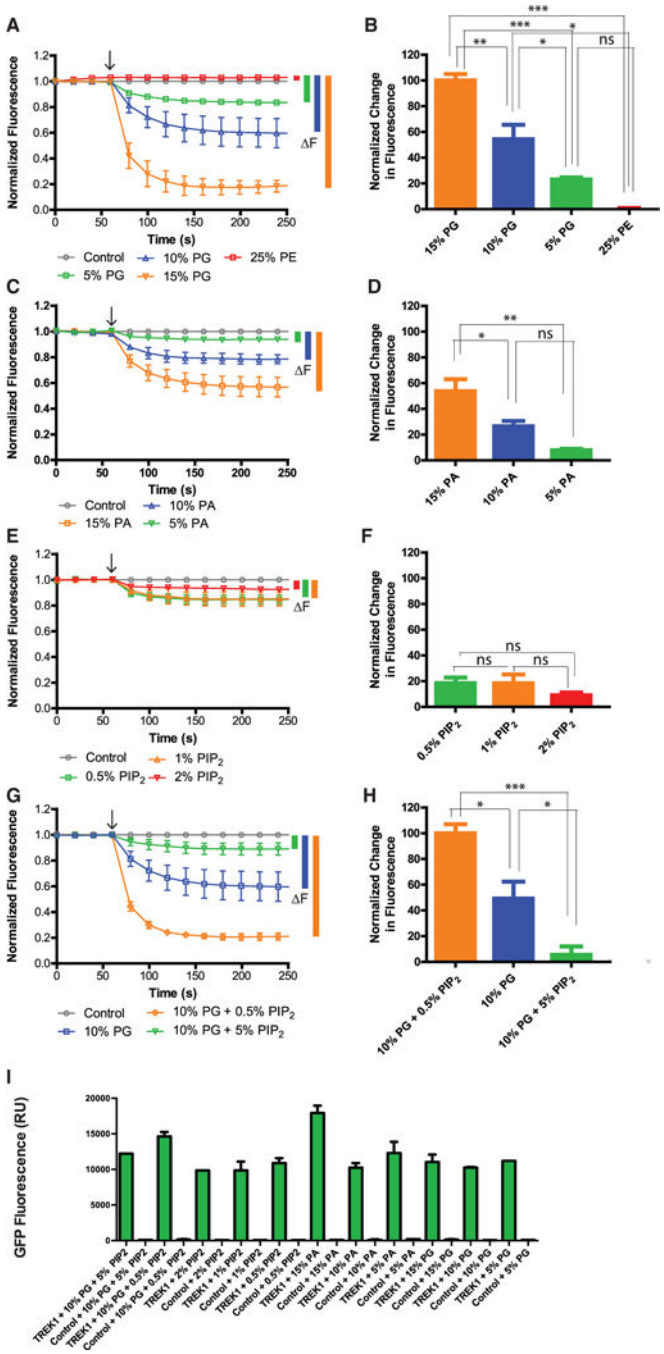

Figure 3. TREK-1 Lipid Gating by Anionic Lipids

Ion flux assays of purified TREK-1 (GFP or Nluc tagged) reconstituted into DOPC proteoliposomes with anionic lipid.

(A) DOPG (PG) dose-dependently agonizes TREK-1, 15% > 10% > 5% (0.81 ± 0.07, 0.43 ± 0.19, 0.16 ± 0.02, respectively, normalized fluorescence). A black arrow indicates the initiation of flux with CCCP. No flux was observed with 25% DOPE (PE) (red trace).

(B) Comparison of end fluorescence shown in (A).

(C) DOPA (PA) also agonizes TREK-1 at 15 and 10 mol% (0.43 ± 0.11 and 0.21 ± 0.05, respectively).
(D) Comparison of end fluorescence shown in (C).
(E) $DOPIP_2$ (PIP_2) fails to activate TREK-1 (0.5, 1, and 2 mol% tested).
(F) Comparison of end fluorescence shown in (E).
(G) Mixtures of PIP_2 and PG (10%) show 5 mol% PIP_2 competes with PG to inhibit TREK-1 (0.11 ± 0.08, normalized fluorescence). Low concentration of PIP_2 in the presence of 10% PG enhanced TREK-1 agonism (orange trace, 0.79 ± 0.04).
(H) Comparison of end fluorescence shown in (G).
(I) Fluorescence emission from TREK1 with a GFP tag after reconstitution into proteoliposomes.
Error bars represent SEM (n = 3–5); no error bar in (I) is a single measurement. ***$p < 0.0001$, **$p < 0.001$, *$p < 0.05$, ANOVA-Tukey's multiple comparison test.

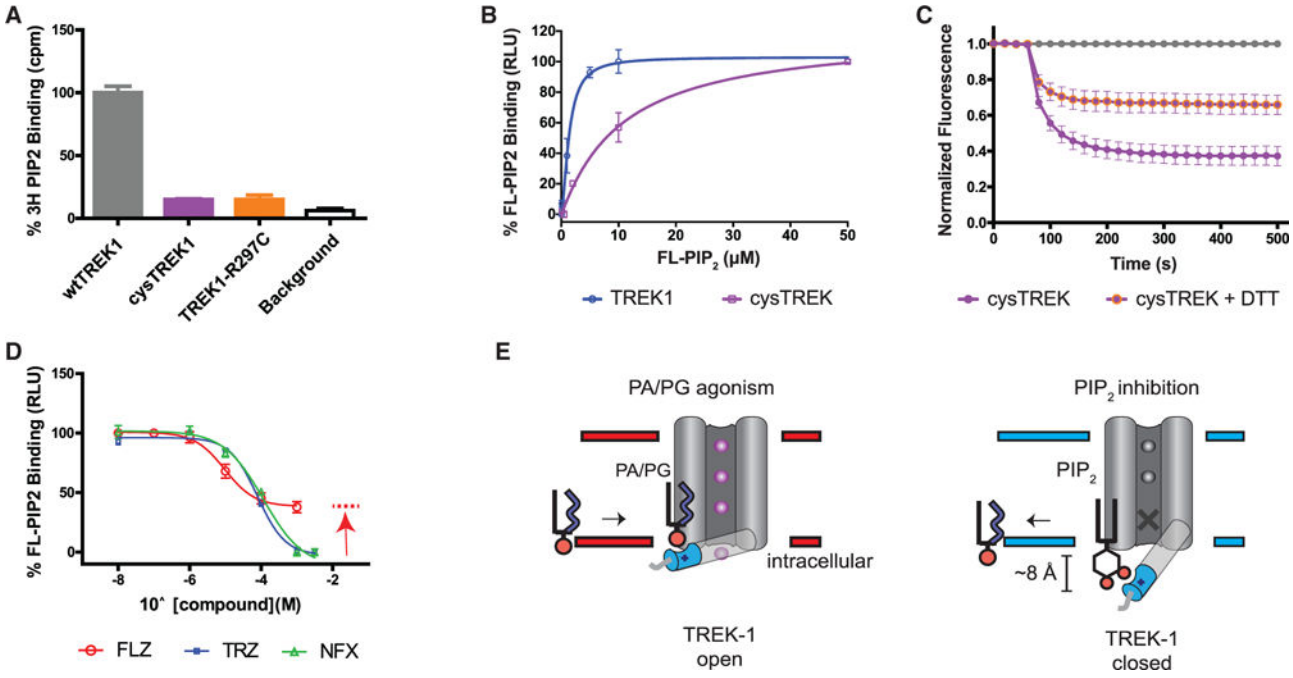

Figure 4. Characterization of the TREK-1 Lipid Binding Site

(A) Cysteine mutants of TREK-1 directly block 500 nM PIP_2 binding. R297 contributes to a known lipid binding site (Chemin et al., 2005), and mutant R297C/F171C (cysTREK) traps an open conformation when disulfide bonded (Brohawn et al., 2014a).

(B) Titration of mutant TREK-1 with FL-PIP_2 results in an ~10-fold decrease in FL-PIP_2 affinity.

(C) Ion flux assay of cysTREK-1 rescues activation in the absence of lipid binding when oxidized (purple trace), but not when reduced with DTT (orange circles); control vesicles are shown as gray circles.

(D) Small molecules fluphenazine (FLZ), thioridazine (TRZ), and norfluoxetine (NFX) dose-dependently compete with FL-PIP_2. FLZ inhibition is incomplete (red arrow and dashed marker) despite a high affinity, K_d of 6.5 ± 2.0 μM. Error bars represent SEM (n = 3–6).

(E) A cartoon showing a proposed model for lipid gating of TREK-1 channels. Anionic lipids PG, PA, and PIP_2 diffuse laterally in the plasma membrane and bind to the channel (a single subunit of TREK is shown). A lipid binding motif (cyan cylinder) extends from the last transmembrane helix of the M4 helix near the inner leaflet of the plasma membrane. (Left) Binding of PA (or PG) to the lipid binding motif causes the tip of the helix to translocate up, activating the channel. A solid red sphere represents the negatively charged head group phosphate. Purple spheres represent ions in the conduction pathway. (Right) PIP_2 displaces PA from the lipid binding site. The geometry of the PIP_2 head group positions the two negatively charged 4′- and 5′-phosphates of PIP_2 (solid red circles) ~8Å away from the membrane compared with PA (the distance of the inositol ring). With PIP_2 bound, the helix adopts a conformation favoring a more closed state of the channel. An X indicates a blocked conduction pathway.

See also Figures S6 and S7.